

AN ACOUSTICAL STUDY
OF
GASES AND VAPORS

By

CHARLES F. SONA

A DISSERTATION PRESENTED TO THE GRADUATE SCHOOL
OF THE UNIVERSITY OF FLORIDA IN
PARTIAL FULFILLMENT OF THE REQUIREMENTS
FOR THE DEGREE OF THE DOCTOR OF PHILOSOPHY

UNIVERSITY OF FLORIDA

1986

ACKNOWLEDGEMENTS

I would like to acknowledge Dr. Sam Colgate for his constant encouragement. His genius has been a source of continuing inspiration.

I would like to express my deepest thanks to my parents who provided the support I needed when I needed it most. Without them, I never would have had the perseverance to accomplish this.

I also would like to express my thanks to Grant Schrag, whose constant comraderie provided me with drive to maintain my sanity in the face of adversity.

Finally, I wish to thank to all of my friends who I have met over the years in Gainesville who have kept me going and helped me enjoy some of the finer places in the beautiful state of Florida.

TABLE OF CONTENTS

	PAGE
ACKNOWLEDGEMENTS	ii
LIST OF TABLES	v
LIST OF FIGURES	vi
ABSTRACT	vii
 CHAPTER	
I INTRODUCTION	1
II ACOUSTICS AND THE SPHERICAL RESONATOR	12
Review of the Equations of Acoustics	12
Eigenvalues and Eigenfrequencies	15
Sound Speed and the Equation of State	25
The Boundary Layer and Other Perturbations	29
Sound Speed in Mixtures	32
The Relaxation Specific Heat	36
III EXPERIMENTAL METHODOLOGY	40
The Resonator, Transducers and Pumping Station	40
Support Electronics	51
Observable and Non-observable Resonances	57
Typical Experiments	60
Relative Measurements	63
Mixtures	65
IV RESULTS	68
Isobutane and n-Butane	68
Estimation of Uncertainties	74
n-Heptane	76

V	CONCLUSION79
APPENDIX		
	LISTING OF BSTAR88
BIBLIOGRAPHY92
BIOGRAPHICAL SKETCH97

LIST OF TABLES

TABLE		PAGE
2.1	Roots of $dj_1(z)/dz = 0$	22
2.2	Radial Mode Resonances of Argon	24
4.1	Sound Speed of the Butanes at Zero Frequency	69
4.2	Ideal Gas Heat Capacities (C_p) of Isobutane and n-Butane70
4.3	Acoustic Second Virials of Isobutane and n-Butane72
4.4	Ideal Gas Reference State Heat Capacity of n-Heptane78

LIST OF FIGURES

FIGURE		PAGE
1.1	Plot of the Resonant Frequencies for the First Radial Mode in Isobutane Versus pressure	10
2.1	The Zero Order Bessel Function j_0	17
2.2	The First Order Bessel Function j_1	19
2.3	The Second Order Bessel Function j_2	21
2.4	The Lennard-Jones (6-12) Potential	28
3.1	12 Inch Diameter Spherical Resonator	42
3.2	Sampling Valve	45
3.3	Cross Sectional View of Acoustic Transducer . .	48
3.4	Vacuum System and Filling Station	50
3.5	System Electronics	53

Abstract of a Dissertation Presented to the Graduate
School of the University of Florida in Partial
Fulfillment of the Requirements for the Degree of
Doctor of Philosophy

AN ACOUSTICAL STUDY
OF
GASES AND VAPORS

By

Charles F. Sona

August 1986

Chairman: S. O. Colgate
Major Department: Chemistry

The measurement of resonant frequencies of radial acoustic standing waves within a gas filled spherical cavity leads to accurate sonic speeds. Because radial modes of vibration have no velocity component tangent to the cavity wall, there are no viscous losses in the sonic speed measurements. Extrapolation of the speed of sound in a gas to zero frequency and zero density permits the calculation of ideal gas reference state heat capacities and acoustic virial coefficients of the sample gas. The physical model relating the resonant frequencies to thermophysical

properties of the gas is presented. The apparatus and experimental procedure are described, and results are given for n-butane and isobutane. A technique which uses argon as a buffer gas allows the procedure to be extended to include studies of vapors of volatile liquids. Results using this technique are presented with data on n-heptane.

CHAPTER I

INTRODUCTION

The thermodynamic equation of state of a gas and the forces which govern the interactions between colliding molecules are intimately related. Once an equation of state is known, all of the predictive power of kinetic theory may be brought to bear on the system of interest. Conversely, the measurement of thermophysical properties of molecules in the gas phase allows for testing of theoretical models of intramolecular forces and indirectly determining the contributions of internal modes of motion of a molecule which are not measurable spectroscopically. Properties which can be measured absolutely such as entropy or heat capacity are particularly well suited for these purposes. This research involves creation of an experimental capability for accurate gas phase heat capacity measurements and test runs to evaluate its performance.

With this end in mind, this work describes an apparatus to measure these quantities of thermodynamic interest. The most powerful aspect of this method is that it allows for the determination of thermochemical properties at the ideal gas reference state of zero pressure. The heat capacity and second acoustic virial coefficient have been determined for isobutane and n-butane in the range of 300 to 350 K and 0.005 and 0.1 M Pa. Some preliminary results for a method of determining heat capacities of high molecular weight vapors are presented. n-Heptane was the vapor used for this study. The data on n-heptane were obtained only at room temperature but the method may be used at any temperature within constraints imposed by the apparatus' design.

In general, experimental measurements of properties of gases and vapors near the zero pressure reference state are both tedious and difficult. By necessity, measurements of properties are made at low to moderate densities and extrapolated to zero density. As the density decreases, however, the magnitudes of the properties under study also become smaller relative to the apparatus and become increasingly more difficult to measure and consequently less reliable. The method of this work uses a system property,

the speed of sound, which is independent of the apparatus features and which can be measured accurately to very low pressures, from which reliable extrapolation to zero pressure may be made.

Alternatively, of course, theoretical calculations may be made on the system of interest. While ab initio quantum mechanical methods offer much promise for the future, present computational aids limit the most accurate calculations to systems of relatively few atoms. Even though statistical thermodynamics theoretically allows for the complete knowledge in theory (1-3), in practice that method still falls short of being fully useful for many systems due to lack of adequate force law information. Too many modes of vibration (torsional and otherwise) are not observed spectroscopically in many systems of practical interest and few theoretical studies of large systems are available. For example, one of the compounds under study in this work, isobutane, a relatively simple system, has only recently had an ab initio quantum mechanical study done on its vibrational modes (4-5). What is even more unfortunate is that the inactive modes are some of the largest contributors for compounds such as hydrocarbons. Thus while theory marches on

and computers become faster and less expensive, it remains necessary to acquire experimental data against which the success of theoretical predictions may be judged.

Thermophysical properties such as heat capacity have been studied by scientists since before the turn of the century. One of the best developed methods is that of vapor-flow calorimetry. Work done by researchers such as Pitzer (6) and Scott and Mellors (7) is exemplary. A good review of the technique may be found in McCullough and Waddington's paper (8). Vapor-flow calorimetry was refined and became a sort of workhorse for the production of thermodynamic data during the forties and fifties. The method became exacting enough to establish values of internal rotational barrier heights (9) and to test models for internal modes in larger molecules (10-13).

Another experimental approach has been based on adiabatic expansion techniques. Early work by Partington (14) used expansion of a gas inside a large carbouy. This work was followed up by Kistiakowski and Rice (15) who improved the method and refined the rather crude apparatus used by Partington. A version of this method is widely used today as a teaching experiment in the physical chemistry

laboratory (16). This method eventually fell into disfavor as improvements in vapor-phase calorimetry and sound speed apparatus led to more accurate determinations of the same properties.

The development of resonance techniques (of which many acoustic techniques may be considered a subset) began in earnest about the same time that vapor-phase calorimetry work was at its peak. Generally, this method employs a piston made of magnetic material set in oscillatory motion by magnetic fields induced in a coil of wire. The resonant frequency is detected by locating the frequency of maximum amplitude of the piston's motion for a given power input (17,18). This technique fell into disfavor as a research tool because of low accuracy; it may, however, be still used in some undergraduate teaching laboratories (19).

"Acoustical motion is, almost by definition, a perturbation" (20, p. 1) Having the knowledge that acoustic wave amplitudes are very small, workers realized that conditions close to thermodynamic equilibrium are maintained, and all properties of the medium remain close to their equilibrium values. This became a powerful reason for workers to begin probing solids, liquids and gases with sonic stimuli. Much

of the early work on sonic studies was concentrated in two main areas: the propagation of sound in free air (21) and air confined in tubes (22,23). As the methods progressed, workers began to study sound propagation in different vapors and at different temperatures (24-26). Work progressed slowly in the field until the development of ultrasonic interferometers increased the accuracy of the technique (27-29). Then, with new developments in microphone technology (30), and theory (31-34), the accuracy of the technique was refined. This continued until the method developed sufficiently that acoustic interferometers could be used for primary thermometric techniques such as establishment of the thermodynamic temperature scale in the 2 to 20 K range (35) and the redetermination of the gas constant R (36,37).

The experimental technique used in this work is a low frequency acoustical one. A sonic field is induced in a spherical cavity of known radius containing the gas or vapor under study and the frequencies of sonic resonance are observed. While it was Rayleigh (38, p. 230) who first developed the theory of the normal modes of vibrational motion in a spherical vessel, later workers such as Ferris

(39) calculated the eigenvalues of the resonator to a higher precision. The first to use a sphere instead of the (then) standard cylindrical interferometer was Bancroft (40). But it was Moldover et al. (41) and Mehl and Moldover (42,43) who developed the technique which allows spherical resonators to be used to collect thermodynamic data of high accuracy. In the present work, their methods are adapted for the study of gases and are extended to provide a source of information on vapors of volatile liquids.

Viscous and thermal boundary losses at the cavity wall are minimized by geometry (the sphere being the shape with the lowest surface area to volume ratio). The wave equation is fully separable and gives a family of solutions, the spherical bessel functions, j_1 , each multiplied by a spherical harmonic. The first solution, j_0 , has purely radial symmetry. A consequence of this is that there is no tangential motion of the gas at the cavity wall and therefore no viscous boundary losses. The lowest observable modes are widely spaced and the frequencies of vibration of practical resonators are typically under 5 kHz. At these frequencies, dispersive effects due to lagging molecular modes are practically nonexistent at working pressures.

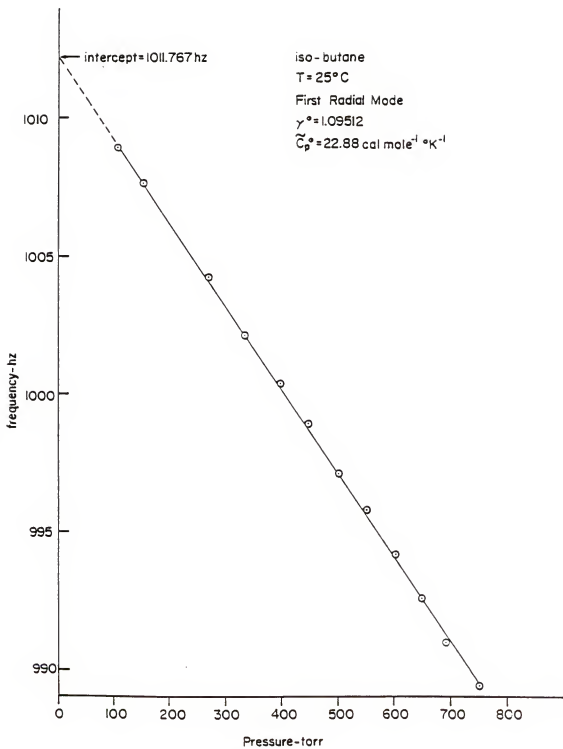
allows for accurate determination of the speed of sound in the gas and therefore of the heat capacity. A typical experiment then involves measuring the resonant frequencies of the gas as a function of temperature, density, and composition (in the case of mixtures).

The most important part of this work is in the study of mixtures of high molecular weight vapors with an inert buffer gas. Because the vapor pressure of the room temperature liquid (n-heptane) is too low to make any direct acoustical measurements, mixtures of the vapor and argon are made. Not only are the amplitudes of the modes now large enough to rise out of the noise, but any problems of lagging internal modes are removed by molecular collision.

A typical experiment involves simply the measurement of the pressure, temperature and frequency of each of the first few radial modes of vibration. A function generator is used to output an acoustic signal to a piezoceramic transducer. The sonic field produces a voltage in an input transducer. This signal is then sent to an envelope detector which produces a D.C. signal proportional to the R.M.S. voltage input to it. At resonance, the amplitude increases dramatically, enabling an exact frequency measurement of the

mode. Using an oscilloscope to locate the vicinity of the maximum signal and a digital voltmeter to find the exact position of the signal peak, resonant frequencies can be found with an accuracy of 0.01 Hz. The temperature is measured simultaneously with frequency. Knowledge of the pressure of the gas inside of the cavity gives a point on the (c,P,T) surface, c being the speed of sound. The temperature is then varied to give the sound speed as a function of temperature at constant density. The density is then varied and resonant frequencies are then again measured at different temperatures. Resonant frequencies were measured at three temperatures: 25, 50 and 75 deg. C and pressures varied between about 600 to 50 torr. At any one given temperature, the frequency varies linearly with pressure, allowing for an extrapolation to the state of zero pressure, the ideal gas reference state. This extrapolation can be done with a high degree of confidence, because of the high degree of linearity of the plot. For example, in isobutane, a plot of the frequency of the first radial mode versus pressure gave a correlation coefficient of 0.99999 (see figure 1.1). It is then concluded that a linear plot sufficiently approximates the behavior of the system.

Figure 1.1
Plot of the Resonant Frequencies
for the First Radial Mode
in Isobutane
Versus Pressure



CHAPTER II

ACOUSTICS AND THE SPHERICAL RESONATOR

Review of the Equations of Acoustics

In this chapter, pertinent equations for the acoustical motion of a gas confined to a spherical cavity are developed. These equations are then related to molecular properties of thermodynamics and kinetic theory. Differences between the first order equations and higher approximations are then treated as perturbations. A discussion on sound speeds in mixtures is then presented.

Consider a gas confined to a spherical container of volume V , a pressure P and at an absolute temperature T in the presence of acoustic excitation. The thermodynamic functions P , T , D (density), E (internal energy), S (entropy), ... etc. may be thought of as consisting of a large static part and a small time dependent acoustic part:

$$\begin{aligned} P &= P_0 + P(t) ; T = T_0 + T(t) ; \\ D &= D_0 + D(t) ; \text{etc.} \end{aligned} \tag{2.1}$$

The objective now is to write dynamic equations of the fluid in terms of the small time dependent part. Since the

acoustic variables are small, all cross terms will be considered to be small and may be regarded as insignificant. Thus, the equations used here are part of what is generally called linear acoustics.

Considering the gas under study (for the moment) as a continuous medium, the Eulerian description of fluid dynamics allows a jumping off point. Consider the acoustical field $\Psi(r, \theta, \varphi)$ produced in a spherical cavity in which r , θ , φ are the positional coordinates. The allowed modes of vibration are given by solving the differential equation first derived by Rayleigh (38, p. 323).

$$\frac{1}{r^2} \frac{\partial}{\partial r} \left[r^2 \frac{\partial \Psi}{\partial r} \right] + \frac{1}{r^2 \sin \theta} \frac{\partial}{\partial \theta} \left[\sin \theta \frac{\partial \Psi}{\partial \theta} \right] + \frac{1}{r^2 \sin \theta} \left[\frac{\partial^2 \Psi}{\partial \varphi^2} \right] = \frac{1}{c^2} \frac{\partial^2 \Psi}{\partial t^2} \quad (2.2)$$

or, more conveniently,

$$\nabla^2 \Psi = \frac{1}{c^2} \frac{\partial^2 \Psi}{\partial t^2} \quad (2.3)$$

where c is the speed of sound in the medium. This is the familiar wave equation for acoustical motion in a lossless fluid. This approximation works quite well for gases at low to moderate pressures and temperatures when the frequency is

not too high. In fact, the magnitude of the two largest perturbations to this theory may be substantially minimized by appropriate experimental design, as will be shown later.

Now perform a separation of variables: Consider the wave function to be of the form $\Psi = R(r)\theta(\theta)\phi(\varphi)e^{-i\omega t}$, ω being the angular frequency, $2\pi\nu$. The φ part becomes a sine or cosine function from the solution of

$$\frac{d^2\phi(\varphi)}{d\varphi^2} = -n^2\phi \quad (2.4)$$

where n must be integral to avoid a discontinuity at $\varphi = 0$ and at 2π . The solution of the theta part may be found by a change of variable to $\cos(\theta)$. Then, after separation of variables, factoring and some rearrangement, the standard form

$$(1-z^2) \frac{d^2\theta}{dz^2} - 2z \frac{d\theta}{dz} + C\theta = 0 \quad (2.5)$$

is found, where $z = \cos(\theta)$. The solutions to (2.5) are the familiar Legendre functions P_m , of order m , where the constant $C = m(m+1)$ and $m=1,2,3,\dots$

All that remains is to solve the radial part of the equation. After constraints imposed by the other parts are invoked, the differential equation becomes

$$\frac{d}{dr} \left[r^2 \frac{dR(r)}{dr} \right] + k^2 r^2 R(r) = m(m+1) ; k = \omega/c \quad (2.6)$$

A solution to (2.6) may be found by setting $x = kr$ and rearranging to the standard form

$$\frac{d^2 R}{dx^2} + \frac{2}{x} \frac{dR}{dx} + [x^2 + m(m+1)] \frac{R}{x^2} = 0 \quad (2.7)$$

For the case in hand, the solutions to (2.7) are known and, for systems not having a discontinuity at the origin, are called spherical Bessel functions, $j_i(x)$. The spherical Bessel function is related to the more familiar ordinary Bessel function $J_i(x)$ by the relation

$$j_i(x) = \sqrt{\frac{\pi}{2x}} J_{i+1/2}(x) \quad (2.8)$$

The functions j_0, j_1 , and j_2 are plotted in figures 2.1-2.3, and values of the first three maxima and minima of each are marked.

Eigenvalues and Eigenfrequencies

The allowed eigenvalues may be calculated by finding the roots of (43)

$$dj_i(kr)/d(kr) = 0 \quad (2.9)$$

Table 2.1 gives the first 80 roots of the functions j_0, j_1, j_2 , etc. However, in this study, only the roots of j_0

Figure 2.1
The Zero Order Bessel Function
 J_0

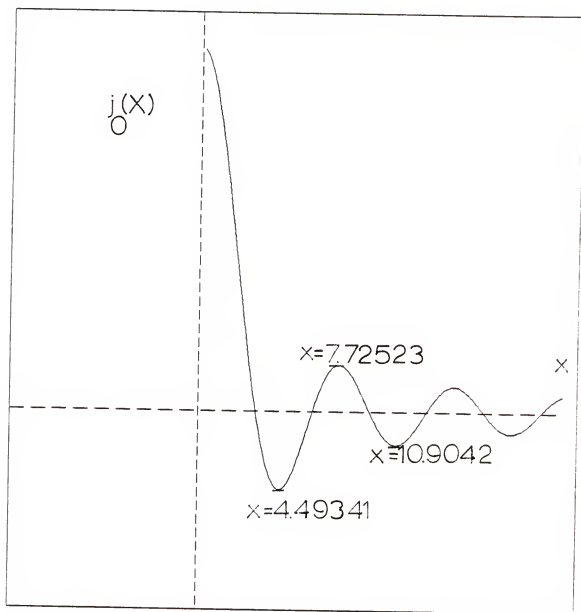


Figure 2.2
The First Order Bessel Function
 J_1

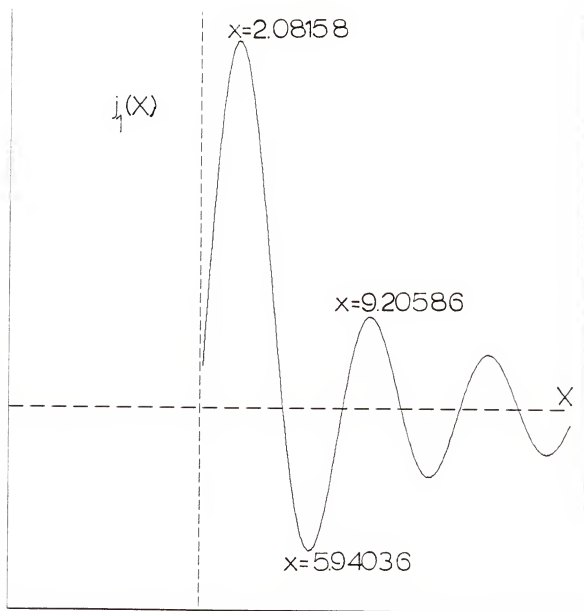


Figure 2.3
The Second Order Bessel Function
 J_2

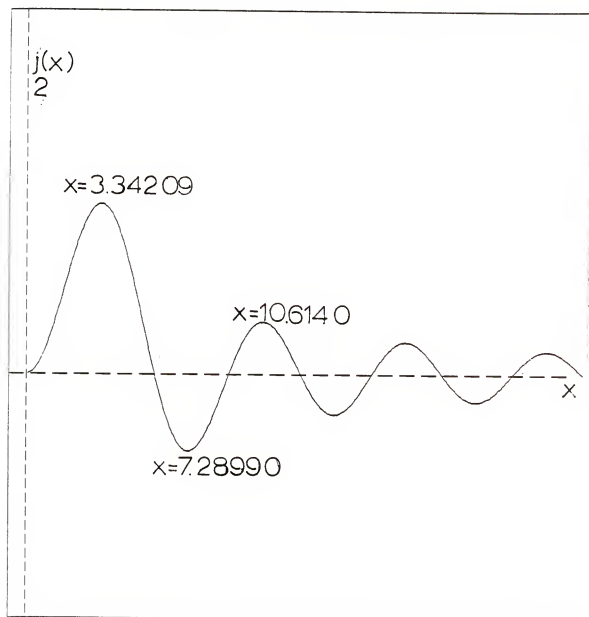


Table 2.1
Roots of $dj_i(z)/dz = 0$

Listed in Ascending Numerical Order					
v	i	n	v	i	n
0.00000	0	0	17.0431	2	5
2.08158	1	1	17.1176	7	3
3.34209	2	1	17.2207	0	5
4.49341	0	1	17.9473	5	4
4.51408	3	1	18.1276	11	2
5.64670	4	1	18.3565	8	3
5.94036	1	2	18.4527	16	1
6.75643	5	1	18.4682	3	5
7.28990	2	2	18.7428	1	6
7.72523	0	2	19.2628	6	4
7.85109	6	1	19.2704	12	2
8.58367	3	2	19.4964	17	1
8.93489	7	1	19.5819	9	3
9.20586	1	3	19.8625	4	5
9.84043	4	2	20.2219	2	6
10.0102	8	1	20.3714	0	6
10.6140	2	3	20.4065	13	2
10.9042	0	3	20.5379	18	1
11.0703	5	2	20.5596	7	4
11.0791	9	1	20.7960	10	3
11.9729	3	3	21.2312	5	5
12.1428	10	1	21.5372	14	2
12.2794	6	2	21.5779	19	1
12.4046	1	4	21.6667	3	6
13.2042	11	1	21.8401	8	4
13.2956	4	3	21.8997	1	7
13.4721	7	2	22.0000	11	3
13.8463	2	4	22.5781	6	5
14.0663	0	4	22.6165	20	1
14.2580	12	1	22.6625	15	2
14.5906	5	3	23.0829	4	6
14.6513	8	2	23.1067	9	4
15.2446	3	4	23.1950	12	3
15.3108	13	1	23.3906	2	7
15.5793	1	5	23.5194	0	7
15.8193	9	2	23.6534	21	1
15.8633	6	3	23.7832	16	2
16.3604	14	1	23.9069	7	5
16.6094	4	4	24.3608	10	4
16.9776	10	2	24.3821	13	3

are of interest. The reason j_0 is chosen may be found in an inspection of the solution to the angular parts of (2.3). All modes of motion in the gas except j_0 have angular dependence. As has been shown by previous workers (43), the modes of purely radial symmetry minimize perturbations introduced by several factors. The advantages of studying radial mode resonances include the following: 1, all modes are resolvable, 2, they have extremely narrow half-widths, 3, resonant frequencies of the radial modes are sensitive to imperfections of non-sphericity only to second order (44,45), and most importantly, 4, viscous damping at the resonator wall does not occur for radial modes. The reason for the last condition enumerated above is that in purely radial mode vibrations there is no tangential motion of the gas with respect to the walls of the cavity.

Once the eigenvalues are calculated for the system, resonant frequencies may be found from

$$f_i = \frac{c \nu_{0i}}{2\pi a} \quad (2.10)$$

where c is the speed of sound in the gas, ν_{0i} are the eigenvalues, and a is the cavity radius. The resonant frequencies of the first 6 radial modes of argon at 25°C in

Table 2.2
Radial Mode Resonances of Argon

ν	f(/sec)
4.49341	1509.20
7.72523	2594.67
10.9042	3662.39
14.0663	4724.44
17.2207	5783.91
20.3714	6842.14

a 12 in. diameter resonator are shown in table 2-2. The speed of sound of an ideal gas may be calculated from knowledge of the heat capacity of the gas. Alternatively, speed of sound data may be used to calculate thermodynamic quantities. The relation between the ratio of heat capacity at constant pressure to the heat capacity at constant volume and the speed of sound is (46)

$$c = \sqrt{\frac{\gamma RT}{M}} \quad (2.11)$$

where R is the gas constant, T is the absolute temperature and M is the molecular weight.

Sound Speed and the Equation of State

For a gas with a non-zero intermolecular potential, (2.11) holds only at zero pressure. Under nonideal conditions, (2.11) may be expanded in a manner similar to that of the virial equation of state. The result, called the acoustic virial equation, takes the form

$$c_0^2 = \frac{\gamma^0 RT}{M} \left[1 + \frac{A(P,T)}{\tilde{v}} + \frac{B(P,T)}{\tilde{v}^2} + \dots \right] \quad (2.12)$$

Here A,B,... are the called the acoustic virial coefficients and are related to the ordinary pressure

virial coefficients. The relation between the second acoustic virial and second pressure virial and its derivatives is (47 p. 232)

$$A = 2B + (2\gamma^0 - 1)T \frac{dB}{dT} + \frac{(\gamma^0 - 1)^2}{(\gamma^0)^2} T^2 \frac{d^2B}{dT^2} \quad (2.13)$$

The second pressure virial coefficient is a function of the intermolecular pair potential $U(r)$ and may be expressed as

$$B(T) = -\frac{2\pi \tilde{N}}{3kT} \int_{r=0}^{r=\infty} r^3 \frac{dU(r)}{dr} e^{-U(r)/kT} dr \quad (2.14)$$

Here \tilde{N} is Avogadro's number, k is Boltzmann's constant, and T is the absolute temperature. It is convenient to define a reduced virial coefficient $B^*(T^*)$:

$$B^*(T^*) = B(T)/b_0 \quad (2.15)$$

where

$$b_0 = \frac{2}{3} \pi \tilde{N} \sigma^3 \quad (2.16)$$

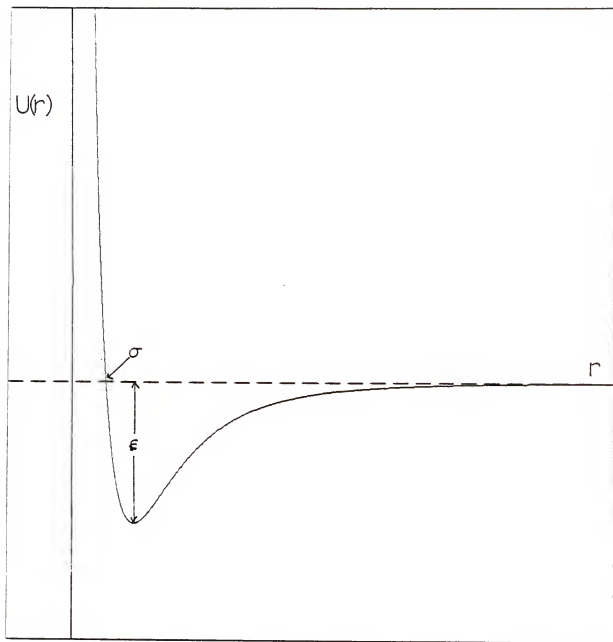
is called the "co-volume" and is equal to 4 times the volume of one mole of rigid spherical molecules.

A much used approximation to $U(r)$ is the Lennard-Jones (6-12) potential,

$$U(r) = 4\epsilon \left[\left(\frac{\sigma}{r} \right)^{12} - \left(\frac{\sigma}{r} \right)^6 \right] \quad (2.17)$$

where ϵ is the well depth and σ is the value of r at which

Figure 2.4
The Lennard-Jones (6-12)
Potential



$U(r)$ crosses the energy axis. If (2.17) is substituted into (2.14) and that into (2.15) and the integration performed, $B^*(T^*)$ is obtained as an infinite series:

$$B^*(T^*) = \sum_{j=0}^{j=\infty} b^{(j)} T^{*-(2j+1)/4} . \quad (2.18)$$

The $b^{(j)}$ are given by

$$b^{(j)} = \frac{-2^{j+1/2}}{4j!} \quad r\left(\frac{2j-1}{4}\right) . \quad (2.19)$$

A plot of the Lennard-Jones (6-12) potential is given in figure (2.4).

Therefore speed of sound data of a gas can yield information about the equation of state and intermolecular forces. Alternatively, a knowledge of intermolecular force constants may permit a calculation of the second acoustic virial coefficient. The computer program BSTAR.BAS given in appendix I calculates $B^*(T^*)$ for temperatures of interest for any gas for which the force constants and heat capacity ratio are known. More information on that program may be found in Chapter IV.

The Boundary Layer and Other Perturbations

Obtaining general solutions to the acoustical equation of motion of a gas with internal energy losses (i.e. heat conduction and viscosity) is an arduous task if started directly from the equations of fluid dynamics. However, if the losses are small, perturbation theory may be applied to Rayleigh's theory to arrive at a meaningful solution.

Consider now the condition of a gas contained in a spherical cavity with a thermal boundary layer at the walls of the cavity. The layer results from heat conduction from the gas into the wall. The wave motion within the body of the gas may be considered to be adiabatic or nearly so, but in the vicinity of the wall may be considered to be isothermal. To compute the shift of resonant frequency caused by this boundary layer perturbation, the following equation (48 p. 562) may be used:

$$4f - ig = \frac{-ic}{2\pi} \frac{\int_s \rho_n^2 \beta \, ds}{\int_v \rho_n^2 \, dv} \quad (2.20)$$

where Δf is the fractional shift in eigenfrequency, ν_n is j_0 and β is the acoustic admittance of the boundary layer. For a wave striking the surface at the normal, the admittance has been shown to be (48 p. 293)

$$\beta = (1 + i) \left[\frac{\gamma - 1}{2\pi a} \right] \sqrt{\frac{\rho \kappa f}{2\pi c C_p}} \quad (2.21)$$

Here a is the radius, γ the heat capacity ratio, κ the thermal conductivity, ρ the density, c the speed of sound, and C_p the constant pressure heat capacity. Inserting (2.21) into (2.20), the resulting shift in resonant frequencies is

$$\Delta f - ig = (1 - i) \frac{\gamma - 1}{2a} \sqrt{\frac{\kappa f}{\rho C_p}} \quad (2.22)$$

This is an extremely important result. Much effort in the design of the present experiment went into minimizing this perturbation. The boundary layer is the largest perturbation to this theory, and some discussion of this equation is merited here. Firstly, the higher the resonant frequency, the larger is the perturbation. Secondly, the larger the diameter of the cavity ($2a$, in the denominator), the smaller the Δf and, just as importantly, the narrower is the resonant peak (the g value), making the exact resonant frequency easier to find. Therefore, the larger the radius,

and the lower the frequencies, the smaller is the halfwidth of the mode. Note also that as $\gamma \rightarrow 1$ this effect becomes negligible. For argon at a frequency of 1.5 kHz a temperature of 25°C and a pressure of 600 torr results in a Δf of approximately .02 Hz or about .001%.

The resonator has holes for evacuation and for the excitation and detection of sound via transducers. They perturb the acoustical field and it is necessary to calculate the change in the eigenfrequencies from them. If an opening has area πr_i^2 and a constant admittance, then from eq. (2.20)

$$\Delta f - i g = \left[\frac{-i c}{8 \pi^2 a^3} \right] \sum_i \pi r_i^2 \beta_i \quad (2.23)$$

The summation is over all holes. Mehl and Moldover (43) give for β

$$\beta_i = -i \cot[kL + (1 + i)\alpha l] \quad (2.24)$$

where α is the "Helmholtz-Kirchoff" attenuation inside the tube connected to the cavity

$$\alpha = \frac{(\pi f)^{1/2}}{(r_i c)} \left[\left[\frac{\eta}{\rho} \right]^{1/2} + (\gamma - 1) \left[\frac{\kappa}{\rho C_p} \right]^{1/2} \right] \quad (2.25)$$

where η and κ are the coefficients of viscosity and thermal conductivity. This perturbation becomes important at some frequencies but is generally negligible, less than .00001%.

Sound Speed in Mixtures

The purpose of this part of the work was two-fold. The first was to determine if an inert buffer gas could facilitate the energy transfer to and from any vibrational modes of a large vapor molecule. The second was to bring up the pressure in the cavity sufficiently to make measurements of resonances possible. The vapor used for this work, n-heptane, has a vapor pressure of about 35 torr at room temperature. Most resonant frequencies typically become unmeasureable in the apparatus when the pressure drops below 50 torr.

Relaxation processes in hydrocarbons have been extensively studied by ultrasonic interferometry (49-54). It is observed that as the frequency of the ultrasound increased, the apparent heat capacity of the molecule becomes smaller and smaller due to lagging flow of energy into and out of modes of vibration. In other words, the period of the high frequency acoustical stress is shorter than the relaxation time of the molecules in that region. This led to numerous

This led to numerous studies of the molecular relaxation rates and calculations of the average number of collisions required to effect a vibration to translation ($v \rightarrow t$) transition. Hertzfeld and Griffing's paper (54) reviews data for several hydrocarbons, and the n-hexane molecule typically took 120 collisions. Unfortunately, no work on n-heptane could be found in the literature. However, the data suggest that as the molecular size goes up, the smaller the number of collisions necessary to effect a transition. It then would be a safe assumption that n-heptane would require about the same number of collisions for a ($v \rightarrow t$) transition.

Richards and Reid (50) found that the most effective species for ($v \rightarrow t$) transitions in hydrocarbons was H_2 . They felt the reason for this was the width of the rotational spacings of H_2 is about the same as that of the vibrational spacings in larger hydrocarbon molecules. Hydrogen's rotational spacing therefore "matched" the vibrational spacings of the hydrocarbon allowing for easier transitions, in effect catalyzing the flow of energy into and out of the hydrocarbon.

If this work were carried out in the ultrasonic range of frequencies, this last fact would be extremely important.

However, in the frequency range of this experiment (less than 10 kHz) the buffer gas need only "be there" as an agent for increasing the pressure of the vapor to make the acoustic signal rise out of the noise. It was hoped that the inert gas would not influence the physical properties of the experimental vapor. Actually, the pressure of the buffer gas was so much higher than that of the vapor that the presence of the vapor could be considered to produce a small perturbation of the sonic speed in the buffer gas. The purpose of using argon is that it would introduce no appreciable quantum effects to the speed of sound in the mixture.

The kinetic theory of gases predicts that the total number of collisions a gas phase molecule makes per second ($Z_{t,A}$) in a mixture of molecules of type A and type B is

$$Z_{t,A} = Z_{AA} + Z_{AB} ; \quad (2.26)$$

Z_{AA} is the collision frequency of type A molecules colliding with themselves and Z_{AB} is the frequency of A colliding with type B. If σ is the effective hard sphere diameter, and n is the number density, the expressions for Z_{AA} and Z_{AB} are

$$Z_{AA} = \left[\frac{4kT}{\pi m} \right]^{1/2} n_A^2 \pi \sigma^2 \quad (2.27)$$

and

$$Z_{AB} = \left[\frac{8kT}{\pi \mu} \right]^{1/2} n_A n_B \pi \sigma_{AB}^2, \quad (2.28)$$

and μ is the reduced mass. For a mixture of argon and n-heptane, at a total pressure of 600 torr, and at 25° C. the total collision rate for each molecule of n-heptane is about 2.0×10^8 per second, about 95% of which are due to argon-heptane collisions. If a sound wave of frequency 10 kHz passes through the medium, local pressure fluctuations occur twice each period or about every 50 microseconds. During that time, a molecule of n-heptane will make about 5000 collisions. It is then concluded that there would be no anomalous dispersion in this instance or for the lower frequency sound waves used in this study.

The Relaxation Specific Heat

The effect of attenuation of acoustical energy by relaxational processes may be understood if the heat capacity is broken down into its components:

$$C_v(\text{Total}) = C_v(\text{trans.}) + C_v(\text{Internal}) \quad (2.29)$$

where $C_v(\text{Trans.})$ is the contribution of the translational

modes and C_v (Internal) of the internal degrees of freedom: rotations, vibrations and electronic contributions. A knowledge of the internal energy levels allows calculation of the thermodynamic properties of the gas. The value of C_v (Trans.) may be taken to be $(3/2)R$, the classical result. Internal modes may be designated by a characteristic temperature. For example, the characteristic temperature of rotation θ_r (55) for a non-linear mode with moment of inertia I is

$$\theta_r = \frac{h^2}{8\pi^2 Ik} \quad (2.30)$$

and θ_r fits into the rigid rotator partition function q_r :

$$q_r = \frac{\pi^{1/2}}{\sigma^2} \left[\frac{T}{\theta_A} \right]^{1/2} \left[\frac{T}{\theta_B} \right]^{1/2} \left[\frac{T}{\theta_C} \right]^{1/2} \quad (2.31)$$

The systems under study all have characteristic temperatures well below room temperatures. Since θ_r is very small, all three rotations are fully activated and the rotational heat capacity is equal to the classical limit of $(3/2)R$. The vibrational and internal rotational modes generally have characteristic temperatures $h\nu_i/k$ at or above room temperature. These modes then are only partially activated. The contribution to the heat capacity of these modes

according to the harmonic oscillator approximation is

$$C_v(\text{vib}) = R \sum_{i=1}^{3N-6} \left[\frac{h\nu_i}{kT} \right] \frac{e^{h\nu_i/kT}}{(e^{h\nu_i/kT} - 1)^2} \quad (2.32)$$

where ν_i is the frequency of the i th vibrational mode. Morse and Ingard (48, p. 296) denote the term in brackets as $F(T)$ in terms of which C_v may be re-written as

$$C_v = R \left[3/2 + 3/2 + 1/2 \sum_n F_n(T) \right] \quad (2.33)$$

where the summation is over all internal rotational and vibrational modes.

If measurements are being made near zero density, then the heat capacity at constant pressure (C_p) and the heat capacity at constant volume are related very simply by

$$C_p = C_v + R \quad (2.34)$$

The heat capacity ratio γ then may be expressed by

$$\gamma = \frac{C_p}{C_v} = \frac{3/2 + 3/2 + 1 + 1/2 \sum_n F_n(T)}{3/2 + 3/2 + 1/2 (\sum_n F_n(T))}$$

(2.35)

If it is next assumed that a degree of vibrational freedom has a characteristic relaxation time, then a dynamic heat capacity may be found to be

$$C_v = C_v(\text{eff.}) + C_v(\text{int.}) \frac{i\omega\tau}{1 + i\omega\tau} \quad (2.35)$$

where $C_v(\text{eff.})$ is called the relaxation specific heat. It

has been experimentally confirmed (see ref.54 for a review of this work) that as the frequency of the sound wave approaches $1/\tau$, the vibrational modes begin contributing less and less to the effective specific heat.

Long chain hydrocarbons have been found to have a "first" relaxation time of on the order of 1×10^{-8} seconds. This means that at high enough pressures and temperatures dispersion of sound does not occur until frequencies of the ultrasound range are reached, typically on the order of 100 KHz. Thusly, it is virtually assured that the heat capacity measured is essentially free from dispersion effects.

CHAPTER III

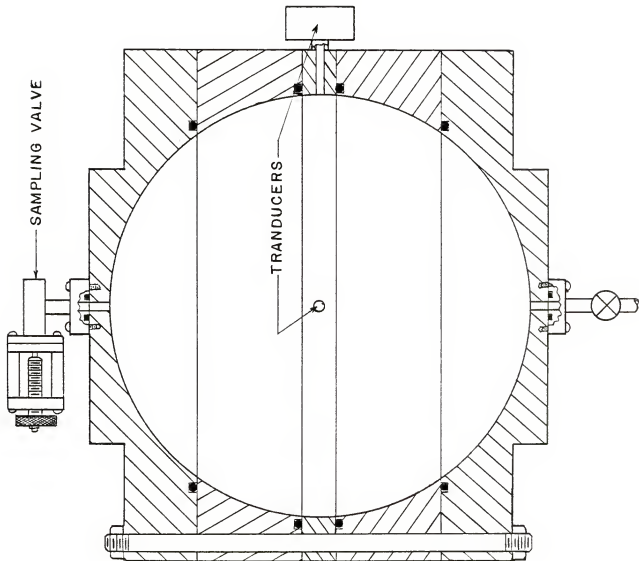
EXPERIMENTAL METHODOLOGY

The Resonator, Transducers, and Pumping Station

The resonator is shown schematically in figure 3.1. The three rings and two end pieces of 15 inch outer diameter are fabricated from 2024 aluminum. The two 1.5 inch diameter brass end caps are attached to valves to allow for filling and evacuating the chamber. Each of these has a six hole 1.125 inch diameter bolt circle and an O-ring gland to accomodate a face seal to the resonator end pieces. The bottom end cap is attached to a sampling valve (to be discussed presently) and the top one to a packless Hoke valve. The latter is used for evacuation and filling of the chamber with permanent gases.

The diameter of the spherical cavity is 12 inches. To ensure sphericity, the cavity was machined as follows. First, each of the five pieces was machined to its exact outer dimensions. Then, O-ring grooves were machined to insure hermetic seals. Next, twelve 3/8 inch diameter holes were drilled in each piece on a 13.5 inch diameter bolt

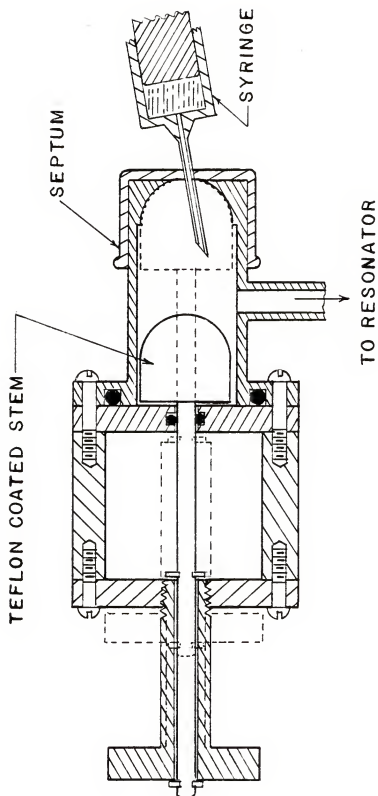
Figure 3.1
12 Inch Diameter
Spherical Resonator



circle. This arrangement assures that sufficient force could be applied to compress the Viton O-rings and maintain stable geometry. Each piece was rough cut internally to a stepped configuration conforming approximately to the final spherical contour. Three of the five parts were then assembled on a fixture and affixed to a lathe. Then the internal surfaces were machined with a 6 inch radius cutter fabricated especially for this purpose. The last step was repeated for the other two sections, and care was taken to move the radius cutter to exactly the same position as before. This way, the entire cavity could be machined to a tolerance exceeding $\pm .0005$ inches or to one part in 12,000.

The sampling valve is shown in cross section in figure 3.2. As noted before, it is used for injecting a known amount of liquid into the system. For operation, a rubber septum closure is first installed over the end of the closed valve. The valve is opened until there is sufficient clearance for a hypodermic needle to be inserted through the septum into the valve body. The liquid is injected (as shown in figure 3-2), and the syringe withdrawn. The plunger is returned to the closed position, and the septum is removed.

Figure 3.2
Sampling Valve



To speed evaporation of fluid in the attaching tubulation, heat is then applied to the valve after injection.

To couple an acoustic wave into and out of the chamber, two transducers are mounted on the center ring of the resonator. They were fabricated in this laboratory using, as their active elements, piezoelectric ceramic bimorphs (Vernitron, Bedford, Ohio) made of material PZT-5H. This ceramic was chosen for its high Curie point (295°C) (56) and high frequency constant (57). A cross sectional view of the transducers is shown in figure 3-3. A sinusoidal voltage is fed in through pins sealed by teflon Wilson seals. To give the bimorph freedom to flex, electrical connections to it are effected with spring contact. Each bimorph is insulated electricially from its aluminum housing by machined teflon supports.

The vacuum system for evacuation and filling the resonator with gases is shown schematically in figure 3-4. A diffusion pump is used to attain a high vacuum inside of the system, after which the resonator may be filled. If pressure measurement with the MacLeod gauge suggested a leak, a helium leak checker is attached to the system and used to

Figure 3.3
Cross Sectional View of
Acoustic Transducer

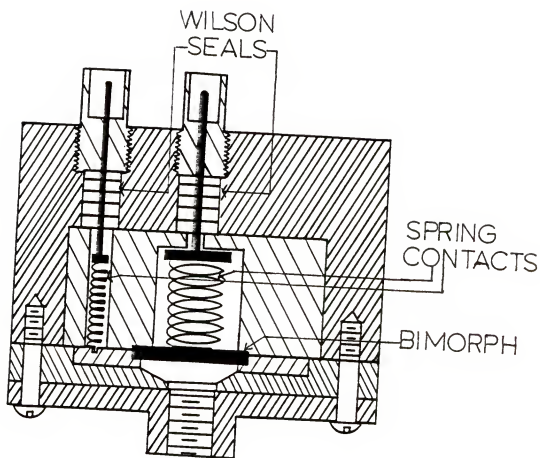
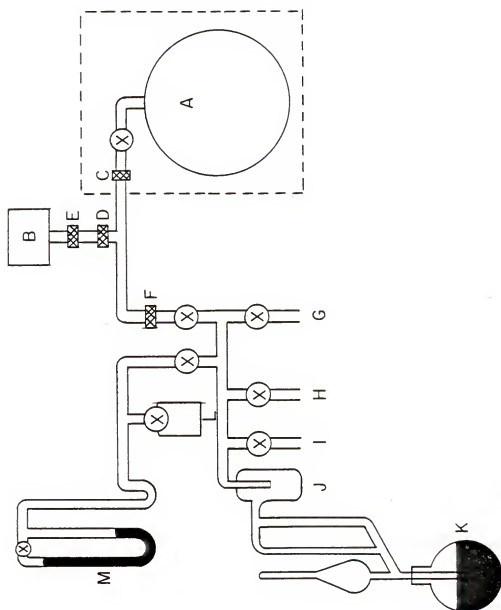


Figure 3.4

Vacuum System and Filling Station

- A. Spherical Resonator inside Isothermal Enclosure
- B. Baratron Pressure Gauge
- C,D,E,F Quick Couples
- G. To Roughing Pump
- H. To Diffusion Pump
- I. To Leak Detector
- J. Cold Trap
- K. McLeod Gauge
- L. Gas Tank
- M. Mercury Manometer

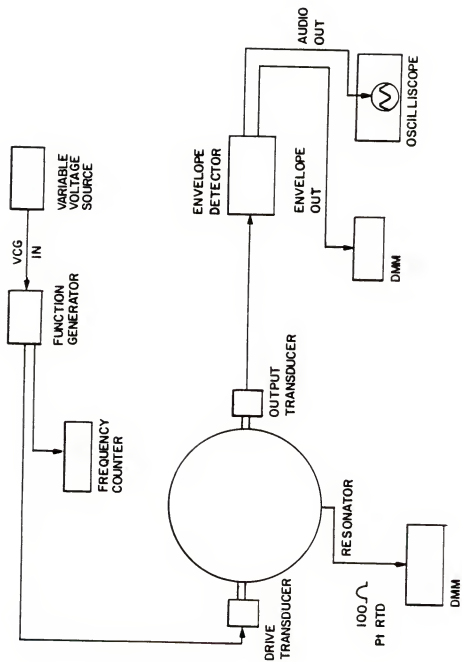


find the leak. Working pressure could be measured by either a capacitive electronic manometer (an MKS Baratron, MKS instruments, Burlington, Mass.) or by a conventional U-tube mercury manometer which was read with a cathetometer. The Baratron has the capability of measuring pressures in the range of .1 to 1000 torr. The cathetometer is accurate to .01 millimeter; however, parallax errors increased the total uncertainty to almost the same order of magnitude as that of the Baratron. To minimize temperature gradients in the system, part of the system is removable so that when evacuation and filling is complete the resonator can be isolated inside of the constant temperature chamber, an industrial oven (Blue M Corp. Blue Island, Ill.), which also supplies heat for the elevated temperature studies of n-butane and isobutane.

Support Electronics

The electronic hardware (shown in figure 3-5) used to operate this experiment can be divided into three main functional parts: firstly, a signal source to provide an

Figure 3.5
System Electronics



acoustical signal, secondly, an output signal measurement system of sufficient accuracy, and finally, temperature and frequency measurement devices. Each will now be discussed in turn.

The primary signal source is a Wavetek (San Diego, Calif) 4MHz function generator, model 182A, variable to 20 Volts peak to peak sine, triangle and square wave output. The function generator has a VCG (Voltage Controlled Generator) input capable of up to 1000 : 1 frequency change with external voltage input of 0 to 4 Volts. Sine distortion is less than .5 % on ranges of frequency used here, also all harmonics are 25 db below the fundamental.

Driving the VCG input of the Wavetek is a variable voltage source fabricated in the departmental electronics shop. To provide for exacting frequency determination, it was necessary for an operator to be able to change the frequency by large intervals (to tune to a frequency near resonance) and to change it by very small intervals (to find the exact center of a resonance). The solution was to build the voltage source with "coarse," "medium," "fine" and "extra fine" controls which output a corresponding voltage. It consists of four operational amplifiers each with a 20

turn variable resistor in its feedback loop. These in turn feed into a summing amplifier in the output section. The total resistance on the feedback loop of the "coarse" control allowed for a full scale output of 4V, for the "medium" amplifier, a full scale output of 0.4V, the fine, 0.04V, and on the "extra fine," .004V. This allowed the operator to change the frequency by amounts of his choosing by simply turning different knobs.

The output section of the system consists of three main parts: an envelope detector, oscilloscope, and a voltmeter. First in line from the output transducer is the envelope detector which also was built in the departmental electronics shops. The first function of this device is to amplify the signal, which could then be displayed on an oscilloscope. Secondly, the envelope detector provides a D.C. output which is read by a voltmeter (Keithley model 177). This way an investigator could tune to a frequency near a resonance, locate the vicinity of the maximum acoustic signal and then search for the maximum to within the accuracy of the voltmeter.

Rounding out the electronics are the pressure, temperature, and frequency measuring devices. The pressure

measuring device, the MKS Baratron, has already been mentioned. The Baratron consists of two functional units. The first is a type 220B absolute pressure gauge. It is of the capacitive type pressure sensor, having a taut metal diaphragm which is made to deflect in response to an applied pressure. The second unit is PDR-D-1 readout which converts the signal output from the gauge into torr. The model 220B has an accuracy of .01% of full scale, \pm one count. System temperature is measured by a 100 Ohm 4-wire platinum resistance thermometer (Hy-Cal Engineering), with $\alpha = .003897 \text{ Ohms/Ohm/Deg.C.}$ and $\delta = 1.5205$ (NBS traceable calibration). The resistance was measured by a Keithley model 195A DVM (Digital Volt Meter). The resolution of the device on the 200 Ohm scale is 1 milliohm. The RTD (Resistive Temperature Detector) is affixed to the outer wall of the resonator by strap clamps holding an aluminum block with a groove of the same dimensions as the RTD. This way good thermal contact with the resonator could be ensured.

At the center of any resonance frequency experiment, there must be a good frequency counter. The one chosen here for this work is a Sencore (Sioux Falls S.D.) FC71, a very high accuracy (NBS traceable calibration) counter.

Below 100 KHz, the device has a resolution of .01 Hz. Another feature of this counter is that it takes only 1/4 of a second to make a measurement, as opposed to other counters which generally require 100 seconds to give .01 Hz resolution. The device uses a crystal which has had its resonant frequency measured as a function of temperature. It senses the temperature of the crystal, looks up the resonant frequency in an EPROM, and calculates the frequency of the external signal from comparison of period measurements of the incoming signal. Thus, unlike conventional counters the FC71 has no oven and requires no warm-up time.

Observable and Non-observable Resonances

For a resonant frequency of the cavity to be measurable the wave must have a finite pressure amplitude at the point of observation. Therefore, a study of the characteristics of the modes of vibration of the chamber itself and of the angular parts of the solution to eq.(2.3) is of a necessity. The solutions to (2.4) and to (2.5) taken together are called the spherical harmonics. The letter l is used to denote successive roots of the Legendre polynomial,

and the letter m to denote each root of eq. (2.4). The allowed values of l are $0, 1, 2, 3, 4, \dots$ and the allowed values for m run from $-l, -l+1, -l+2, \dots, 0, \dots, l-2, l-1, l$. The roots of most concern in this paper have spherical symmetry; that is, $l=m=0$. One important point of interest is that the lowest root of j_0 is at zero, which corresponds to zero frequency and is of course unmeasurable. It can simply be attributed to the zero of wave energy, the gas at rest. Table 2-1 lists the first 80 roots of $dj_i/dr=0$. These values may be found either in the literature (39,58) or may be calculated numerically. The actual functionality of successive functions can be calculated from the recurrence relation (58)

$$[(2i + 1)/z]j_i(z) = j_{i-1}(z) + j_{i+1}(z) \quad (3.1)$$

and the first two functions j_0 and j_1 are (59)

$$j_0 = \sin(z)/z, \quad j_1 = \sin(z)/z^2 - \cos(z)/z, \quad (3.2)$$

from which the rest may be calculated. Inspection of table 2.1, a list of the first 80 eigenvalues of $dj_i/dz=0$, will show that the first observable radial resonance $\nu=4.49341$ is very close numerically to the (3,1) mode $\nu=4.5108$ (A convention used in naming resonances will be to name them by the Bessel functions order then the number of the root). An

inspection of the Legendre polynomial of order 3 which is written as

$$P(\theta) = 1/8(5\cos(3\theta) + 3\cos(\theta)) \quad (3.3)$$

reveals a nodal surface at 90 degrees from maximum intensity of the polynomial. For this reason it was decided to position the sound transducers at right angles to each other. The (0,1) mode came through very well and the (3,1) mode was suppressed sufficiently so that deconvolution was not necessary. Using an x-y plotter attached to the envelope detector and driven by the output transducer generates a graphical representation of the resonant signal. The difference in intensity of the (0,1) mode and (3,1) mode indicated that no deconvolution schemes were necessary to separate the signal centers.

The apparatus itself has intrinsic modes of vibration. Using the x-y plotter on the evacuated chamber gives many apparatus modes, the first one occurring at about 1700 Hz. The resonant frequencies of this apparatus mode and its first harmonic have several very important characteristics: First, they are weakly temperature dependent and shift slowly with temperature and therefore tend to stay in about the same frequency region; second, they are extremely

decoupled from the gas resonances, evidenced by the fact that these cavity modal resonances do not shift when the resonator is evacuated or filled. Another property of these apparatus vibrations is that the symmetries of radial resonances of the gas and of the resonator structure are so radically different that the resonances will be decoupled anyway.

Typical Experiments

Now that a description of the apparatus has been made, a description of routine measurements can be addressed. Extremely high purity argon gas (Matheson, 99.9995%) is admitted into the evacuated resonator. The pressure and temperature are allowed to equilibrate and are subsequently measured. Then, the resonant frequencies of the first 6 radial modes are recorded. The temperature is determined at the time of each frequency measurement using the Platinum RTD. This gives one point on the (f, T, P) surface. The temperature is raised to the vicinity of the next set point, and the chamber is allowed to equilibrate again. The new frequencies of the same six eigenvalues are now measured.

The temperature is finally raised to the last set point, and the frequencies are once again measured. Collection of a full data set at one pressure typically took most of one day; so overnight the system was allowed to cool back to room temperature. The next morning the frequencies of the same modes were again measured to determine if any leaks or outgassing occurred during the temperature cycle. Outgassing of the walls is generally characterized by a small shift in the frequencies which becomes smaller with each successive pump-down, while leaks are characterized by a continuous drift in frequency. If no leaks or outgassing problems were observed, some of the gas in the system was pumped out and the new pressure was measured. The frequencies were then again measured at the same three temperatures. If a leak occurred, the system was leak checked and the problem fixed. If outgassing occurred, a new sample of gas was pumped into the system.

Once a particular frequency has been measured, the frequency can be normalized to a reference temperature. The three reference temperatures of this study are 25, 50 and 75 degrees Celsius. If g_n denotes the ratio of the measured frequency of the n th radial mode to its corresponding

eigenvalue, then by equation (2.10),

$$c_n^2 = 4\pi^2 a_T^2 g_n^2 \quad (3.4)$$

where c is the speed of sound and a_T is the diameter of the resonator at temperature T . It was found through many experiments with argon that the g value of each radial eigenvalue is, to within experimental error, independent of frequency. Therefore, it is safe to assume that $c_n = c_0$, the sound speed at zero frequency. Inserting equation (2.11) for c_0 and taking the differential change of g value with temperature it is found

$$dg = \left[\frac{\gamma^0 R}{8\pi^2 a_T^2 T} \right]^{1/2} dT \quad (3.5)$$

(3.5) or approximately,

$$\Delta g = \left[\frac{\gamma^0 R}{8\pi^2 a_T^2 T} \right]^{1/2} \Delta T \quad (3.6)$$

But Δg may be rewritten as

$$\Delta g = \frac{f(T + \Delta T) - f(T)}{\nu} \quad (3.7)$$

where $f(T)$ is the frequency at the reference temperature and $f(T + dT)$ is the frequency at the temperature the measurement is made at. Once normalization is complete, the perturbations mentioned in chapter II are subtracted off. This yields the corrected frequencies for argon, which are

used for calibration of the resonator and for relative measurements, discussed in the next section.

Relative Measurements

The gases isobutane and n-butane (Phillips, 99.99 %, and 99.96 %) were studied by making relative measurements. All of the above relationships given in the past two chapters are absolute equations. All equations assume that the gas vibrates independently of the all modes of the chamber itself, that is to say it has been assumed that the gas moves independently of the outside world. Of course that is not strictly true. No theory can accommodate all unknowns, but by making all calculations relative to some standard system, with physical properties which are well documented, the effect of many of these variables may be removed from the picture. The standard system used in this work is pure Argon gas. Use of this gas is a sort of double edged sword, however. While the properties of the gas are well known, Argon has the largest perturbation from the boundary layer effect (see equation 2.22). If $g_{i,Ar}$ is defined as the ratio of the frequency of the i th resonance

to its eigenvalue in Argon, then from eqs. (2.10) and (2.12),

$$c_{i,Ar}^2(P,T) = 4\pi^2 a^2 g_{i,Ar}^2 = \frac{\gamma_{Ar}^0 RT}{M_{Ar}} \left[1 + \frac{A(T)_{Ar}}{V_{Ar}} \right] \quad (3.8)$$

where $C_{i,Ar}$ is the sound speed of Argon at the pressure and temperature of measurement. If the subscript x denotes an experimental gas, then

$$c_{i,x}^2(P,T) = 4\pi^2 a^2 g_{i,x}^2 \quad (3.9)$$

Dividing (3.9) by (3.8) gives

$$c_{i,x}^2 = c_{i,Ar}^2 \left[\frac{g_{i,x}}{g_{i,Ar}} \right]^2 \quad (3.10)$$

which may also be written as

$$c_{i,x}^2(P,T) = \left[\frac{f_{n,x}}{f_{n,Ar}} \right]^2 \frac{\gamma_{Ar}^0 RT}{M_{Ar}} \left[1 + \frac{A_{Ar}(P,T)}{V} \right] \quad (3.11)$$

Since the departure from ideality is very small at operating pressures and temperatures in this study, the infinite series was truncated at the second term. Using this method, the speed of sound was then calculated as a function of temperature and pressure. At each temperature and each pressure, the speed of sound at zero frequency is then calculated from extrapolation to zero frequency.

The speed of sound is then extrapolated down to zero density giving finally the sonic speed at zero pressure and

at zero frequency, which is the ideal gas reference state.

The heat capacity at constant pressure is then

$$C_p = \frac{\gamma^0}{\gamma^0 - 1} R \quad (3.12)$$

Heat capacities of n-butane and isobutane, determined by this method, are listed in table 4-2.

Mixtures

This section develops the equations necessary for the determination of heat capacities of dilute solutions of low vapor density compounds in an inert gas solution. The experiment measures shifts in radial mode frequencies from those of pure argon caused by the injection of small amounts of the vapor.

Since the mole fractions of sample gas used in this work are small, assume that a solution of the vapor in argon is ideal; equations (3.1) and (2.11) can be combined to give

$$c^2 = 4\pi^2 a^2 \left[\frac{f_n}{\nu_{01}} \right]^2 = \frac{\gamma(P,T,X)RT}{M_X} \quad (3.13)$$

where X is the mole fraction of the sample vapor, and M_X is the average molecular weight

$$M_X = X_1 M_1 + X_2 M_2 \quad (3.14)$$

If the vapor behaves ideally, then C_p and C_v for argon are

then $5/2R$ and $3/2R$ and γ then becomes

$$\gamma = \frac{C_p(P,T,X)}{C_v(P,T,X)} = 1 + \frac{1}{(C^* - 1.5)X + 1.5} \quad (3.15)$$

where C^* is a "reduced" heat capacity, C_v/R . Experimental values of γ are then determined from (3.10) and are related to pure argon frequencies $f_{0,n}$ measured at the same temperature by

$$\gamma^0 = \frac{5}{3} \frac{M_x}{M_{Ar}} \left[\frac{f_n}{f_{0,n}} \right]^2 \quad (3.16)$$

Gamma of the vapor may be evaluated as follows. The resonant frequencies are measured as a function of composition. A plot of $1/[\gamma(P,T,X) - 1]$ versus X is then made. Rearrangement of eq.(3.12) yields

$$1/[\gamma(P,T,X)-1] = (C^*-1.5)X + 1.5 \quad (3.17)$$

which should be a straight line with intercept 1.5 and a slope equal to $C^* - 1.5$, if the assumptions made are justified. As will be seen in the next chapter, no systematic changes with frequency were found thereby confirming the assumptions as satisfactory in the present study.

In this chapter, the experimental apparatus has been described and pertinent equations for data reduction

derived. In the next chapter, the results of the experiments that were performed will be presented.

CHAPTER IV

RESULTS

Isobutane and n-Butane

The sonic speeds of isobutane and n-butane have been calculated at 25, 50, and 75 degrees Celcius at pressures between 50 and 600 torr from data obtained by measurement of the resonant frequencies of the first 6 radial modes of vibration. Linear least squares analysis using equations developed in chapter III were used to find the speed of sound at zero frequency. These results are presented in table 4-1. These data were then plotted against density and were extrapolated to zero pressure. In accordance with the physical model presented in Chapters II and III, this extrapolation permits the evaluation of the heat capacity in the ideal gas reference state. Table 4-2 shows the heat capacity values that were calculated using methods outlined in this work, and values obtained by other workers (60-62). It is evident that the room temperature values obtained in

Table 4-1
Sound Speed of the Butanes at Zero Frequency

T = 25 deg. C

N-Butane

I-Butane

P(torr)	c(m/s)		P(torr)	c(M/s)	
49.91	215.43	±.02	50.1	215.65	±.02
102.52	215.11		99.8	215.40	
199.87	214.35		200.70	214.67	
301.32	213.72		300.28	214.01	
399.60	213.03		400.00	213.41	
498.50	212.35		499.30	212.74	

T = 50 deg. C

P(torr)	c(m/s)		P(torr)	c(m/s)	
108.50	223.49	±.04	108.02	223.72	±.04
215.54	222.63		217.13	222.98	
325.04	222.16		326.18	222.37	
432.44	221.55		430.41	221.78	
541.90	220.94		542.99	221.23	

T = 75 deg. C

P(torr)	c(m/s)		P(torr)	c(m/s)	
232.21	230.67	±.07	116.09	231.84	±.07
350.19	230.32		233.93	230.93	
465.90	229.83		351.41	230.44	
581.60	229.18		454.95	229.86	
			585.00	229.34	

Table 4-2
Ideal Gas Heat Capacities (C_p) of Isobutane and n-Butane

C_p (J/K-mole)				
T(Deg.C)	This work	Chen(a)	Rihani (b)	Whacker (c)
<u>Isobutane</u>				
298.15	96.40 \pm 0.02	96.65	97.02	96.78
323.15	102.34 \pm 0.05	103.51	104.22	103.56
348.15	107.45 \pm 0.09	110.41	111.17	110.36
<u>n-Butane</u>				
298.15	98.84 \pm 0.02	98.58	100.70	
323.15	105.06 \pm 0.05	104.93	107.24	
348.15	114.02 \pm 0.08	110.41	113.60	

a) Statistical mechanical calculations using a combination of experimental and theoretical parameters; see reference 60,
 b) Group contribution method, see reference 61, c) Flow calorimetric method. See reference 62

this study agree well with the literature, but the values at elevated temperatures show some discrepancy. This can be attributed principally to relatively poor temperature control at the elevated temperatures. This problem will be minimized in future work following major changes in the temperature control system.

Table 4-3 lists values of the second acoustic virial coefficients obtained by other workers (63,64) and by the following method. The density of the gas was first approximated by the ideal gas law; then a straight line fit of c^2 versus density was made. From eq. (2.12), the intercept a is

$$a = -\frac{\gamma^0 RT}{M} \quad (4.1)$$

and the slope b is

$$b = -\frac{A(P,T)}{M} - \frac{\gamma^0 RT}{M} \quad (4.2)$$

The second acoustic virial, $A(P,T)$, is therefore equal to the intercept divided by the slope, times the molecular weight:

$$A(P,T) = Mb/a \quad (4.3)$$

Next, an iterative procedure was used to find a best fit of the least squares coefficients a and b . If a truncated virial equation is assumed,

Table 4.3
Acoustic Second Virials
of
Isobutane and n-Butane

Gas	T (deg.K)	A(cm ³ /mole)		
		A (this work)	A(a) Haynes et.al.	A(b) (Theo.)
isobutane	298.15	-1130 ±1	-1131	-907
	323.15	-1019 ±1	-945	-794
	348.15	-969 ±2	-860	-700
n-butane	298.15	-1085 ±1	-1214	-1173
	323.15	-1013 ±1	-1010	-1030
	348.15	-794 ±2	-860	-916

a) See references 63 and 64.

b) Using the program BSTAR and force constants taken from ref. 47 pg.1112.

$$\tilde{P}\tilde{V} = RT(1 + B(T)/\tilde{V}) \quad ; \quad (4.4)$$

\tilde{V} , the molar volume, can also be calculated from a trial value of $B(T)$. The density is recalculated from the new value of the molar volume, and the sonic speed data refitted to the new densities. The first trial value for $B(T)$ was taken from values of ϵ/k and b_0 tabulated in Hirschfelder et al. (47, p.1112). This value also corresponded to a value of $B(T)$ which was used to calculate a new density, and a linear regression was once again performed. Unfortunately, the only values obtainable for force constants for isobutane were deduced from viscosity data, which led to a poor starting value for that gas. This is in keeping with the general observation that force constants obtained from transport phenomenon measurements often agree poorly with those obtained from equation of state data. A linear regression was performed on the speed of sound data. This procedure was repeated until the best fit to these data was found, yielding finally the second acoustic virial coefficients.

The theoretical calculations of $B(T)$ and $A(P,T)$ were made using the program BSTAR.BAS listed in appendix I. Even though the calculation of $B(T)$ based on the Lennard-Jones (6-12) potential involves a gamma function, no numerical

integration scheme was necessary. A property of the gamma function is that

$$\Gamma(n+1) = n\Gamma(n) \quad (4.5)$$

It was found that for all values of n , the argument of the gamma function had a fractional part of either .25 or .75. A loop calculated the product of all terms except $\Gamma(1.25)$ or $\Gamma(1.75)$, which in turn were obtained from standard mathematical tables.

Estimation of Uncertainties

Since the data obtained from these experiments were fitted to a straight line, it is necessary to calculate the uncertainties of a linear least squares fit. The uncertainty in the least squares line $y = mx + b$ is given by (65)

$$\lambda(m) = \left[\frac{N}{D} \right]^{1/2} \lambda(y) \quad (4.6)$$

and

$$\lambda(b) = \left[\frac{\sum x_i^2}{D} \right]^{1/2} \lambda(y) \quad (4.7)$$

where the summation is over the experimental data points,

and where D is

$$D = N \sum x_i^2 - (\sum x_i)^2. \quad (4.8)$$

The uncertainty in the frequency measurement of the counter was ± 0.01 Hz and the uncertainty in pressure measurement over the full range is never greater than 0.2 torr. From

eqs. (2.10) and (2.11), the approximate formula

$$c_1/c_2 = (T_1/T_2)^{1/2} \quad (4.9)$$

can be used to calculate an uncertainty in c from an uncertainty in c . At 25 degrees C, thermocouple measurements at the top and bottom of the resonator typically differed by less than 0.05° C. At 50° C, this difference rose to about 0.12° C; at 75° C, it was 0.2° C. These uncertainties in temperature were used to calculate the uncertainties shown in table 4.1. Inserting these values into equations (4.3) and (4.4), the uncertainties in the parameters a and b were calculated for each run. The uncertainty in the acoustic virial coefficient was then given by

$$\lambda^2(A) = A^2 \left[\lambda^2(b)/b^2 + \lambda^2(a)/a^2 \right] \quad (4.10)$$

To calculate the uncertainty in the heat capacity ratio γ , it is first necessary to consider the uncertainty propagated in the formula

$$\gamma = c_0^2 M / RT \quad (4.11)$$

which is found to be

$$\lambda^2(\gamma) = \gamma^2 \left[\lambda^2(c_0)/c_0^2 + \lambda^2(T)/T^2 \right] \quad (4.12)$$

The calculated uncertainty in C_p is then

$$\lambda^2(C_p) = C_p^2 \left[2 \lambda^2(\gamma)/\gamma^2 \right] \quad (4.13)$$

The uncertainties in C_p are listed in table 4.2.

n-Heptane

The vapor n-heptane was studied by the method of mixtures outlined in chapter III. The speed of sound data were collected only at room temperature in this study but the apparatus is being modified so that work on mixtures can be extended to elevated temperatures. Additional work will appear as modifications of the apparatus are completed.

Resonant frequencies of mixtures of argon mixed with gravimetrically determined amounts of n-heptane were used to plot a line from equation (3.17). From data taken at 0.1 MPa, and at 298° K, a C_p of 164.4 ± 0.8 J/mole-K was calculated from equations given in the last section of chapter III. This value is compared to values obtained by other workers in table (4.4), which range from 155.56 to 175.27. The good agreement with the calculations of Scott (66) and with those of Person and Pimentel (67), using group contribution methods based upon statistical mechanical principles and limited spectroscopic data, originally devised by Pitzer (68), suggests that the method used is quite successful. The other data are presented in table (4.4) is based on empirical group contribution methods of known low reliability. The agreement between the good quality

theoretical results and the data in this work tends to confirm the newly developed gas mixture technique as a viable method for the determination of heat capacities of vapors of low vapor densities.

Table 4.4
Ideal Gas Reference State
Heat Capacity
of
n-Heptane

C_p (J/ mole - K)

This Work

164.4 +/- .8

165.18 Scott, ref. 66

165.98 Person and Pimentel,
ref.67

175.27 Spencer and Flannagan,
ref.68

173.30 Rihani and Doriaswami,
ref.61

155.56 Pitzer, ref.69

CHAPTER V

CONCLUSION

The small amplitudes of acoustic wave motion make sonic techniques ideal for the study and measurement of thermo-physical properties of gases. While earlier work with sound waves utilized primarily the ultrasonic range, the technique of the present study is in the audible range of frequencies. The speed of sound was measured as a function of temperature, pressure, and frequency. This allowed for an accurate extrapolation of the measured quantities to both zero frequency and zero density, which is the ideal gas reference state. The thermodynamic quantity obtained by this method was the ideal gas reference state heat capacity which is a property of much thermodynamic interest in both basic and applied science.

From fundamental acoustical relationships, it is found that the acoustical wave equation is fully separable for a boundary of spherical symmetry. In a system with no discontinuity at the origin, the solution of the wave equation leads to a family of functions, which consist of a

spherical Bessel function, multiplied by a spherical harmonic. The solution of the boundary value constraint $(d\psi/d(kr))_{r=a}$, where a is the radius, provides a series of eigenvalues which can be used to relate the speed of sound in the gas to the observed frequencies.

Corrections to the simple theory can be made using perturbation theory. The two largest corrections are for the boundary layer and for the non-zero coupling of the spherical cavity resonances with the small tubulations connected to the cavity. Both of these corrections are made smaller by the design of the cavity. Since the zero order Bessel function has no velocity component tangent to the cavity wall, the viscous contribution to the boundary layer is absent. The other correction due to the thermal conductivity is proportional to $f^{1/2}$, and since the cavity is of a relatively large dimension (12 inches), and f is characteristically smaller, that contribution is correspondingly smaller. In the case of the connecting tubulations, their frequencies of resonance are typically much higher than those of the radial modes under study and are decoupled from the radial vibrations.

A preliminary experiment involving a mixture of an inert buffer gas with vapors of a high molecular weight liquid of moderately low vapor pressure was undertaken. The buffer gas served a twofold purpose: first, to increase the pressure within the cavity to make the resonances observable, second, to facilitate the transfer of energy to and from any lagging modes of vibration in the vapor molecules. Ultrasonic interferometry measurements have shown that the average number of collisions necessary to produce a vibration to translation transition for n-heptane is on the order of 10^2 . Arguments based on collision rate theory show that the number of collisions occurring during the passage of one half-wave of 10 kHz frequency is much greater than the number of collisions necessary to effect a transition. Thus it is inferred that the heat capacity measured in this experiment should be error free due to lost contributions.

A 12 inch diameter spherical resonator was constructed in the departmental shops and used to test these theories. The resonator consists of five aluminum pieces with a spherical inner contour. Attached to the center ring are two sonic transducers using bimorphs as their active elements.

The two transducers are positioned at 90° to each other. This arrangement permitted measurement of the frequency of the lowest radial mode without interference of the nearby (3,1) mode. Valves are attached to the top and bottom of the resonator. The bottom valve allows for the injection of gravimetrically determined amounts of a liquid. The top valve permits connection of the resonator to a gas filling station, pressure gauge and high vacuum system. The vacuum system was designed so that the resonator could be evacuated and then filled with a permanent gas. Pressure was measured by either a manometer or by a McLeod gauge.

The primary signal source used in this study was a 4 MHz function generator. To control frequency output, a variable voltage source was used to generate a voltage determined by the settings on the controls of the device. Monitoring the frequency of the function generator is a frequency counter of very low drift and very high accuracy.

Receiving the signal from the output transducer is an envelope detector, which connects to several devices. These include an oscilloscope, for tuning to the vicinity of a resonance and a digital voltmeter for tuning to the exact center of the resonance. Whenever a resonant frequency was

measured, so also was the temperature, using a platinum RTD. Resonant frequencies were then corrected to the reference temperature.

The heat capacity and acoustic virial coefficients of the gases isobutane and n-butane have been measured at 25, 50, and 75° C. The values obtained are listed in table (4.2). The method used was as follows. First, the resonant frequencies of the radial standing wave were measured at each temperature and pressure. The chamber was then evacuated and a sample gas admitted into the chamber. The resonant frequencies of the same modes of vibration were then measured in the sample gas at approximately the same temperatures and pressures. The values of the speed of sound were computed relative to the values obtained in pure argon. Extrapolation to zero pressure finally yielded ideal gas reference state sonic speed, from which the heat capacity ratio was determined. From the slope of this line, the value of the acoustic virial coefficient was also determined.

To extend the range of measurement of the speed of sound to higher and lower temperatures than those used in this study will be a major undertaking. Accurate temperature measurements remains the most difficult challenge in these

sonic speed measurements, and uncertainties in the temperature are bound to increase unless steps are taken to provide an isothermal enclosure of superior design. Another problem facing high temperature measurements is the development of suitable high temperature acoustic transducers. High temperature insulation and poor high frequency performance are the principal problems with the use of electromechanical devices. Piezoelectric devices must be used well below their Curie points and are thus useless above about 500 K. One possible solution to be explored in this laboratory involves the use of modulated laser beams interacting with absorbent materials to generate acoustical waves and other laser beams reflected from thin diaphragms to detect the sound waves.

Spherical resonators can provide a plethora of thermophysical information. Although the only properties measured in this work were heat capacity and second acoustic virial coefficient, there are other properties that can be studied with this technique. Planned improvements in the apparatus will open the door to these expanded studies. For example, studying behavior of the acoustic virial coefficient as a function of temperature and pressure can lead to information about the pressure virial coefficients. From these,

information about the intermolecular potential may be deduced, and applying the technique to gas mixtures can result in experimental determination of the potential between unlike molecules. Reacting gas systems may also be studied by monitoring the shift of the resonant frequency of a mode of vibration as the reaction proceeds. It may also be possible to study the vapor pressure of a liquid as a function of temperature thereby obtaining information on the heat of vaporization of the liquid.

Another possible use for the spherical resonator is in the measurement of vibrational and rotational relaxation times of gas phase species. Much work is being done in this field utilizing optoacoustic and purely spectrophotometric techniques. Both methods utilize a laser to pump molecules into a specific excited electronic state. The molecules then undergo internal conversion to highly excited vibrational states. The molecules then collisionally lose their energy either by collisions with the other molecules (typically an inert buffer gas) or by internal conversion. The rate of loss of the excited species is either monitored by the production of an acoustic signal or by the loss in absorption of light characteristic of the excited species.

The optoacoustic technique provides information about only vibrational to translational and rotational to translational transitions, while the spectroscopic technique cannot distinguish between these and vibrational to vibrational quenching. But, using the two methods in conjunction with each other can provide for a more complete description of relaxation pathways.

The resonator used in the present study could be modified for photoacoustic measurements. There are many advantages of using this apparatus for this type of work. First, the corrections to Rayleigh's theory of acoustics are known to a high degree of accuracy and may be treated by perturbation theory. Second, for a spherical resonator, the bulk viscosity of the medium perturbs only the half width of a resonance, and not the frequency of the resonance (the bulk viscosity is the macroscopic manifestation of relaxation phenomena). Third, all resonant frequencies of the radial modes are resolvable, making deconvolution of resonant peaks unnecessary. Since the bulk viscosity can be measured by the halfwidth of a radial mode, a signal analyzer can be used to filter out all frequencies except those near the resonance of interest. Then the voltage

produced as a function of frequency in the vicinity of the resonance could be recorded. By subtracting all other perturbations, a value of the bulk viscosity can be determined, from which a value of the relaxation time may be extracted.

It is the author's hope that the present work will mark the beginning of a vigorous new program in this laboratory using acoustic resonance measurements to explore a variety of interesting gas phase thermophysical properties.

APPENDIX

LISTING OF BSTAR

Below is listed the program BSTAR.BAS, which will calculate the reduced second virial coefficient $B(T^*)$ given a value of the reduced temperature, T^* . BSTAR.BAS also calculates the first and second derivative of $B(T^*)$. This code also calculates the reduced second acoustic virial coefficient $A(T^*, \gamma)$, from an inputted value of γ .

```
10 REM
20 REM C.Sona 4/17/86
30 REM BSTAR.BAS calculates reduced second virial
35 REM coefficients
40 REM and acoustic virials from tstars and gammas.
50 REM for more information and pertinent equations see HCB
55 REM pg.163 for more details
60 REM
70 DEFDBL B
80 DEFDBL F,Z,A
90 DEFDBL N,T,Q,G,P
100 INPUT "input tstar";TSTAR
```



```

110 INPUT "gamma"; GAMMA
120 G1FORTH=.9064024771#
130 G3FORTH= .9190625268#
140 FAK=2
150 PROD=1
160 A=1.2254167024#
170 B=3.625099082#
180 B0=(2^.5)*A*TSTAR^-.25
190 B1=-1*(2^1.5)*(B/4)
200 B1=B1*TSTAR^(-.75)
210 B2=-1*(2^(2.5))
220 B2=B2*(A/8)*TSTAR^(-1.25)
230 BZERO=B0+B1+B2
240 B1STAR=B0*(-.25) - .75*B1 -1.25*B2
250 B2STAR= .25*1.25*B0 + .75*1.75*B1 + 1.25*2.25*B2
270 FOR J=3 TO 50
280 NEWTOT=BZERO
290 N=(2*J-1)/4
300 FAK=FAK*J
310 REM
320 REM this calculates the b(j) terms
330 REM

```

```
340 PROD=1
350 Z=N-INT(N)+1
360 IF Z=1.25 THEN 400
370 PROD=PROD*G3FORTH
380 GOTO 410
390 REM
400 PROD=PROD*G1FORTH
410 REM this calculates the rest of the gamma function
420 JZ=N
430 IF JZ-Z =0 THEN 470
440 PROD=PROD*(JZ-1)
450 JZ=JZ-1
460 GOTO 430
470 Q=J+.5
480 PROD=-1*PROD*(.25)*(2^(Q))/FAK
490 TS=TSTAR^(-1*(2*J+1)/4)
500 ZIP=PROD*TS
510 BZERO=BZERO+ZIP
520 Q1=ZIP*-.25*(2*J+1)
530 B1STAR=B1STAR+Q1
540 B2STAR=B2STAR -.25*Q1*(2*J+5)
550 IF ABS(NEWTOT-BZERO)<1E-10 THEN 580
```

```
560 PRINT J,BZERO
```

```
570 NEXT J
```

```
580 ASTAR= 2*BZERO + 2*(GAMMA-1)*B1STAR +  
(GAMMA-1)^2*B2STAR/GAMMA
```

```
590 PRINT BZERO,B1STAR,B2STAR,ASTAR
```

```
600 END
```

BIBLIOGRAPHY

1. L. S. Kassel, Chem. Rev. 18, 277 (1936)
2. K. S. Pitzer, Chem. Rev. 27, 39 (1940)
3. J. A. Beattie, Chem. Rev. 44, 141 (1949)
4. A. T. Hagler, P. S. Stern, S. Lifson and S. Ariel,
J. Amer. Chem. Soc. 101, 813, (1979)
5. C. D. Chalk, B. G. Hutley, J. McKenna, L. B. Sims, and I.
H. Williams, J. Amer. Chem. Soc. 103, 261 (1981)
6. K. S. Pitzer, J. Am. Chem. Soc. 63, 2413 (1941)
7. R. B. Scott and J. W. Mellors, J. Res. Natl. Bur. Stand.
34, 243 (1945)
8. J. P. McCullough and G. Waddington, "Experimental
Thermodynamics", ed. J. P. McCullough and D. W. Scott
Vol. I, Ch 10., Plenum Press, New York, 1968.
9. W. Weltner Jr. and K. S. Pitzer, J. Am Chem. Soc. 73,
2606, (1951)
10. K. S. Pitzer, J. Chem. Phys. 8, 711 (1940)
11. K. S. Pitzer and W. D. Gwinn, J. Chem. Phys. 10, 428
(1942)
12. K. S. Pitzer, J. Chem. Phys. 14, 239 (1946)
13. J. E. Kilpatrick and K. S. Pitzer, J. Chem. Phys. 17,
1064 (1949)
14. J. R. Partington, Proc. Roy. Soc. A100, 27 (1922)

15. G. B. Kistiakowski and W. W. Rice, J. Chem. Phys. 7, 281 (1939)
16. D. P. Shoemaker, C. W. Garland J. I. Steinfeld, "Laboratory Experiments in Physical Chemistry", McGraw-Hill, New York, 1974.
17. A. L. Clark, L. Katz, Can. J. Research A, 18, 22 (1941)
18. L. Katz, S. B. Woods, and W. F. Leverton, Can. J. Res. 27, 27 (1949)
19. D. G. Smith, Am. J. Phys 47, 593 (1979)
20. P. M. Morse and K. Uno Ingard, "Encyclopedia of Physics" XI/1, ed. by S. Flugge, Spriger-Verlag, Berlin, 1961.
21. M. E. Delanay, Acustica 38, 201 (1977)
22. Lord Rayleigh, "Theory of Sound"; Vol. I, 2nd Ed. Dover New York, 1956
23. A. Kundt, Pogg. Ann. 127, 497 (1868)
24. E. H. Stevens, Ann. d. Phys. 7, 285 (1902)
25. A. Kalahne, Ann. d. Phys. 11, 225 (1903)
26. Dixon, Cambell and Parker, Proc. Roy. Soc. 100, 1(1922)
27. A. Telfair, W. H. Pielemeier, Rev. Sci. Instrum. 13, 122 (1942)
28. K. F. Hertzfeld, F. O. Rice, Phys. Rev. 31, 691 (1928)
29. D. G. Bourgin, Nature 122, 133 (1928)
30. W. Kuhl, G. R. Schodder, F. K. Schroder, Acustica 4, 519 (1954)
31. H. L. Saxton, J. Chem. Phys. 6, 30 (1938)

32. D. G. Bourgin, Phys. Rev. 50, 355 (1935)
33. D. Bancroft, Am. J. Phys. 24, 35 (1956)
34. J. H. Connolly, J. Acoust. Soc. Amer. 36, 2374 (1964)
35. A. R. Colclough, Metrologica 9, 75 (1973)
36. T. J. Quinn, A. R. Colclough, and T. R. Chandler,
Philos. Trans. Roy. Soc. London 283, 367 (1976)
37. A. R. Colclough, Proc. Roy. Soc. London Ser. A 365, 125
(1979)
38. Lord Rayleigh, "Theory of Sound"; 2nd Ed. Dover New
York 1956 vol. II, sect.230
39. H. G. Ferris, J. Acous. Soc. Amer. 4, 57 (1952)
40. D. Bancroft, Amer. J. Phys. 24, 355 (1956)
41. M. R. Moldover, M. Waxman, M. Greenspan, High Temp. High
Press. 11, 75 (1979)
42. J. B. Mehl, M. R. Moldover, Proc. of 8th Sympos. on
Thermophys. Prop. Pub. by A.S.M.E. New York, (1981),
43. J. B. Mehl, M. R. Moldover, J. Chem. Phys. 74, 4062
(1981)
44. J. D. Campbell, Acustica 5, 145 (1955)
45. J. B. Mehl, J. Acoust. Soc. Amer. 71, 1109 (1982)
46. G. N. Lewis and M. Randall, revised by K. S. Pitzer and
L. Brewer "Thermodynamics"; McGraw-Hill, New York,
1961, pg. 109
47. J. O. Hirschfelder, C. F. Curtiss and R. B. Bird, "The
Molecular Theory of Gases and Liquids", John Wiley and
Sons, New York, 1954.
48. P. M. Morse and K. U. Ingard, "Theoretical Acoustics",
McGraw-Hill, New York, 1968 eq. 9.4.14, pg. 562
49. D. G. Bourgin, Phys. Rev. 50, 355 (1936)

50. W. T. Richards and J. A. Reid, J. Phys. Chem. 2, 206 (1934)
51. J. C. McCoubrey, J. B. Parke, A. R. Ubbelohde, Proc. Roy. Soc London A233, 155 (1955)
52. M. E. Jacox, S. H. Bauer J. Phys. Chem. 61, 833 (1955)
53. T. D. Lambert and R. S. Rowlinson, Proc. Roy. Soc. London A204, 424 (1951)
54. K. F. Hertzfeld and V. Griffing, J. Phys. Chem. 61, 844 (1955)
55. T. L. Hill, "Statistical Thermodynamics"; Addison-Wesley, Reading, Mass. 1960.
56. "Modern Piezoelectric Ceramics", Vernitron Inc, Bedford, Ohio, n.d.
57. "Piezoelectric Technology Data For Designers", Vernitron Inc., Bedford, Ohio, n.d.
58. Mathematical Tables Project, National Bureau of Standards, "Tables of Spherical Bessel Functions"; Cambridge University Press, New York, 1947
59. P. M. Morse and H. Feshbach, "Methods of Theoretical Physics"; McGraw-Hill Book Co., New York, 1953, part 1 pg. 622
60. S. S. Chen, R. C. Wilhoit and B. J. Zwolinski, J. Phys. Chem. Ref. Data 4, No. 4, 859-69
61. D. N. Rihani and L. K. Doriaswami, Ind. Eng. Fundam. 4, 17-21 (1965)
62. P. F. Wacker, R. K. Cheney and R. B. Scott, Journal of Research of the National Bureau of Standards, Research Paper RP1084 38, 651 (1947)
63. W. M. Haynes and R. D. Goodwin, Nat. Bur. Stand. (U.S.) Monograph 169 (Apr. 1982).

64. R. D. Goodwin and W. M. Haynes, Nat. Bur. Stand. (U.S.)
Tech. Note 1051 (Jan. 1982)
65. P. R. Bevington, "Data Reduction and Error Analysis for
the Physical Sciences"; McGraw-Hill, New York, 1969
pg.113.
66. D. W. Scott, J. Chem. Phys. 60, 3144 (1974)
67. W. B. Person and G. C. Pimentel, J. Am. Chem. Soc.
75, 532 (1953)
68. H. M. Spencer and G. N. Flannagan, J. Am. Chem. Soc.
64, 2511 (1942)
69. K. S. Pitzer, J. Chem. Phys. 8, 711-20 (1940)

BIOGRAPHICAL SKETCH

Charles Sona was born on October 16 1958, in Union, New Jersey. His family moved to Freehold, New Jersey, in 1974, where he attended Freehold Regional High School and graduated from there in 1976. Deciding that he enjoyed science, he chose to pursue a degree in chemistry and enrolled at Fairleigh-Dickinson University in Madison, New Jersey, in the same year. Before graduating, he found that he received no pleasure working as a synthetic chemist and decided that it was not his calling in life. He graduated from FDU in 1980 and decided to continue studies in physical chemistry at the University of Florida, where he has been ever since.

I certify that I have read this study and that in my opinion it conforms to acceptable standards of scholarly presentation and is fully adequate, in scope and quality, as a dissertation for the degree of Doctor of Philosophy.

Samuel O. Colgate
Samuel O. Colgate, Chairman
Associate Professor of Chemistry

I certify that I have read this study and that in my opinion it conforms to acceptable standards of scholarly presentation and is fully adequate, in scope and quality, as a dissertation for the degree of Doctor of Philosophy.

John P. Eyler
John Eyler
Professor of Chemistry

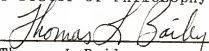
I certify that I have read this study and that in my opinion it conforms to acceptable standards of scholarly presentation and is fully adequate, in scope and quality, as a dissertation for the degree of Doctor of Philosophy.

Willis Person
Willis Person
Professor of Chemistry

I certify that I have read this study and that in my opinion it conforms to acceptable standards of scholarly presentation and is fully adequate, in scope and quality, as a dissertation for the degree of Doctor of Philosophy.

Gus Palenik
Gus Palenik
Professor of Chemistry

I certify that I have read this study and that in my opinion it conforms to acceptable standards of scholarly presentation and is fully adequate, in scope and quality, as a dissertation for the degree of Doctor of Philosophy.



Thomas L. Bailey
Professor of Physics

This dissertation was submitted to the Graduate faculty of the Department of Chemistry in the College of Liberal Arts and Sciences and to the Graduate School and was accepted as partial fulfillment of the requirements for the degree of Doctor Philosophy.

August 1986

Dean, Graduate School